Structural Eng./Earthquake Eng., JSCE, Vol. 13, No. 1, 29s—41s, 1996 April

NUMERICAL IDENTIFICATION OF SECONDARY BUCKLING PHENOMENA OF ELASTIC RECTANGULAR PLATE UNDER PURE BENDING†

Masatoshi NAKAZAWA[1], Kiyohiro IKEDA[2], Satoshi WACHI[3] and Shigeru KURANISHI[4]

[1]Member of JSCE, Dr. Eng., Lecturer, Dept. of Civil Eng., Tohoku Univ. (Sendai 980-77, JAPAN)
[2]Member of JSCE, Ph.D., Professor, Dept. of Civil Eng., Tohoku Univ.
[3]Member of JSCE, M. Eng., NKK Corporation (Yokohama 230, JAPAN)
[4]Member of JSCE, Dr. Eng., Professor, Kanto-Gakuin Univ. (Yokohama 236, JAPAN)

In this paper, the secondary buckling phenomena of the elastic rectangular plate subject to pure bending moments are investigated. The bifurcation points are classified numerically based on the determinant of tangential stiffness matrix and of its diagonal blocks obtained by means of the group-theoretic bifurcation theory. With reference to these blocks within the whole block-diagonalized one, the informations of the instability points and equilibrium paths after bifurcation are easily obtained. The quantitative influence of the initial imperfections are investigated based on the asymptotic laws and Monte Carlo simulations.

Key Words : *Instability, secondary buckling, bifurcation-point classification, numerical identification, block-diagonalization technique, path tracing, rectangular plate*

1. INTRODUCTION

It is a well-known fact that the initial or primary buckling of an elastic perfect plate is generally a stable symmetric bifurcation from the initially undeflected equilibrium state. However, the behavior beyond buckling is not investigated in full detail, because this type of problem generally has higher-order nonlinearities. Such an elastic plate retains the sufficient resistance against external loads even beyond the primary buckling and has been thought to be stable and to show monotonical behavior in the post-buckling range.

As for the large deflection problems of the elastic plate, Levy[1] solved von Kármán's fundamental equations for a simply-supported square plate under the edge compression combined with lateral pressure. Coan[2] solved Marguerre's fundamental equations with the effect of small initial curvature to generalize the Levy's solution. Yamaki[3] also solved Marguerre's equations under eight different conditions which include two kinds of loading conditions and four kinds of supporting ones. The solutions by Levy and Coan can be treated as special cases of these results. From these studies, it has also been well known that the post-buckling behavior of a plate becomes complicated owing to the two-dimensional property which yields the highly-mixed harmonic patterns in the deformed configuration.

In some experimental and theoretical studies on the post-buckling behaviors of a rectangular plate subject to the in-plane uniaxial compression: e.g. Bauer and Reiss[4], Sharman and Humpherson[5], Chilver[6], Uemura and Byon[7),8] and Supple[9),10),11], it has been revealed that a plate deformed in a primary buckling mode may snap abruptly to another configuration with a different pattern of deflection. This phenomenon is called the secondary instability or secondary buckling. Nakamura and Uetani[12] progressed the theoretical investigation for the secondary buckling and post-secondary behaviors by the multi-terms coupling effect of buckling modes. Unstable and stable symmetric bifurcation points on the secondary branching paths are observed, and the snap-through motions involving an abrupt change of wave-form are presented.

† This paper is translated into English from the Japanese paper, which originally appeared on J. Struct. Mech. Earthquake Eng., JSCE, No.519/I-32, pp.67–78, 1995.7.

Recently, Maaskant and Roorda[13] studied the post-buckling behavior of a simply-supported plate under combined loading of biaxial compression. This interaction of loadings leads to the mode jumping phenomenon associated with the secondary bifurcation, and the characteristics of mode coupling in the buckling modes are investigated for several loading conditions.

However, few researchers pointed out the existence of instability except for the case under compressive load. Fujii and Ohmura[14] reported that in the elastic FEM analysis of a panel of the curved girders, some numerically unstable points exist at which a large number of iterations are required to obtain a converged answer. We believe that this is also the secondary instability phenomenon, but this kind of unstable mechanism has not been focused on up to now.

Recently, we[15)~17] found out that a flat plate subject to the pure bending indicates the snap-through or bifurcation type instability phenomena even beyond the primary buckling. Furthermore, similar behavior is observed in the case of unequal bending and shear loading. Moreover, we revealed the mechanism of bifurcation hierarchy of a simply-supported plate under pure bending by the group-theoretic bifurcation theory[18].

Ref. 18) focuses the theoretical background of secondary bifurcation, while this paper emphasizes the aspects of numerical analysis and mechanism of the secondary buckling phenomena. The equilibrium paths are obtained by both load-control and displacement-control type analysis, and numerical identification of the bifurcation points are carried out by relatively simple operation[19)~21] based on the determinant of those tangential matrices. Based on the bifurcation hierarchy[18] obtained by group-theoretic bifurcation theory, more detailed classification of bifurcated paths and bifurcated points is carried out.

Since the post-buckling behavior of them becomes generally stable, engineering concern will be to decide the allowable limit of deflection. In this paper, the method of analysis to obtain the post-buckling behavior and that of evaluation of deflection are suggested, based on several methods of analysis[19)~21] and findings[22)~24] by the bifurcation theory. When the deflection is relatively small, we evaluate it by the asymptotic equation in the vicinity of stable symmetric bifurcation point. On the other hand, large deflection is evaluated by the post-buckling analysis with initial imperfections using the Monte Carlo simulation. As was described, the establishment of a numerical method which makes possible to trace correctly the complicated post-buckling behavior of a plate is also a very important problem.

2. DERIVATION OF FUNDAMENTAL EQUATIONS

The large deformation theory is adopted to trace the post-buckling behavior of a flat plate. It must be noticed that the nonlinear differential equations by von Kármán-Marguerre with initial deflection will be applied up to the thickness order of plate deflection.

Four sides simply-supported (4s.s.) and two opposite sides clamped and the other two sides simply-supported (2c. & 2s.s.) boundary conditions are adopted for a rectangular plate as the analytical models of this study. The fundamental equations are formulated under the action of uniaxial pure bending moment.

(1) Differential equations for large deflection

Kármán-Marguerre's equations[17] with initial deflection are expressed in terms of the out-of-plane deflection $w(x,y)$, initial deflection $w_o(x,y)$ and the in-plane stress function $F(x,y)$ as

$$\nabla^4 w = \frac{t}{D}\left[\frac{\partial^2 F}{\partial y^2}\frac{\partial^2(w+w_0)}{\partial x^2}+\frac{\partial^2 F}{\partial x^2}\frac{\partial^2(w+w_0)}{\partial y^2} -2\frac{\partial^2 F}{\partial x\partial y}\frac{\partial^2(w+w_0)}{\partial x\partial y}\right], \quad (1a)$$

$$\nabla^4 F = E\left\{\left[\frac{\partial^2(w+w_0)}{\partial x\partial y}\right]^2 -\frac{1}{2}\left[\frac{\partial^2(w+w_0)}{\partial x^2}\frac{\partial^2(w+w_0)}{\partial y^2} +\frac{\partial^2(w+w_0)}{\partial y^2}\frac{\partial^2(w+w_0)}{\partial x^2}\right] -\left(\frac{\partial^2 w_0}{\partial x\partial y}\right)^2+\frac{1}{2}\left[\frac{\partial^2 w_0}{\partial x^2}\frac{\partial^2 w_0}{\partial y^2}+\frac{\partial^2 w_0}{\partial y^2}\frac{\partial^2 w_0}{\partial x^2}\right]\right\} \quad (1b)$$

where t and $D \equiv Et^3/12(1-\nu^2)$ are the plate thickness and the flexural rigidity of the plate, respectively. E is Young's modulus and ν is Poisson's ratio. In order to ensure the symmetric order of differentiation in the series expansion, Eq. (1b) is modified in some parts from that of well-known type. The in-plane stress components $\sigma_x(x,y)$, $\sigma_y(x,y)$ and $\tau_{xy}(x,y)$ are related to the Airy stress function $F(x,y)$ as

$$\sigma_x = \frac{\partial^2 F}{\partial y^2}, \qquad \sigma_y = \frac{\partial^2 F}{\partial x^2}, \qquad \tau_{xy} = -\frac{\partial^2 F}{\partial x\partial y} \quad (2)$$

This stress function $F(x,y)$ must be determined to satisfy the loading condition. We here consider the pure bending moments M as the external load, then the mechanical boundary conditions given by the stress resultant forces can be

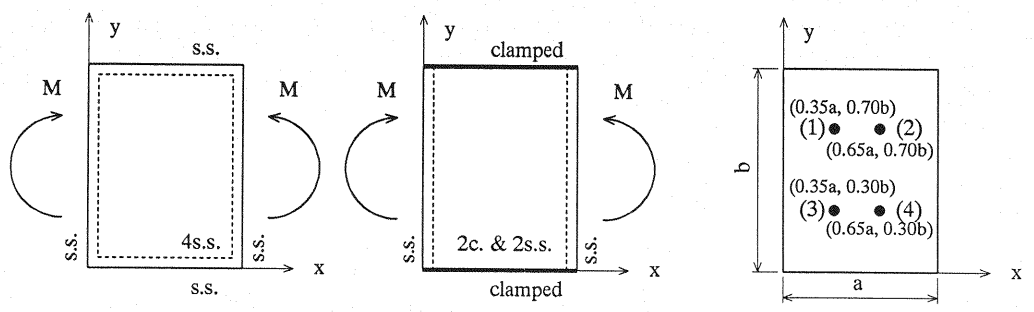

Fig. 1 Boundary condition of a rectangular plate and observation points of out-of-plane deflection

expressed as

$$M = -t\int_0^b \sigma_x(x,y)(y-\frac{b}{2})dy, \quad \text{for } x=0,\ a, \tag{3a}$$

$$\int_0^b \sigma_x dy = 0, \quad \text{for } x=0,\ a, \tag{3b}$$

$$\int_0^a \sigma_y dx = 0, \quad \text{for } y=0,\ b, \tag{3c}$$

$$\tau_{xy} = 0, \quad \text{for } x=0,\ a \text{ and } y=0,\ b \tag{3d}$$

These boundary conditions of Eqs. (3a~3d) can be exactly satisfied if a homogeneous solution of Eq. (1b) is chosen for the Airy stress function[15].

$$F_0(y) = -\frac{y^2(2y-3b)}{b^3 t}M \tag{4}$$

(2) Simply-supported rectangular plate

The deflections can be expressed for the four edges simply-supported conditions as

$$w_0 = t\sum_{m=1}^{\infty}\sum_{n=1}^{\infty} a_{mn}\sin\left(\frac{m\pi x}{a}\right)\sin\left(\frac{n\pi y}{b}\right), \tag{5a}$$

$$w = t\sum_{m=1}^{\infty}\sum_{n=1}^{\infty} b_{mn}\sin\left(\frac{m\pi x}{a}\right)\sin\left(\frac{n\pi y}{b}\right) \tag{5b}$$

where a_{mn} are the given quantities of initial deflection, and b_{mn} are the unknown coefficients to be determined. m and n are the number of half harmonic waves in the $x-$ and $y-$ directions, respectively. The general expression of $F(x,y)$ is obtained by summing a particular solution corresponding to the right-hand side of Eq. (1b) using Eq. (5), and the homogeneous solution $F_0(y)$ of Eq. (4) as

$$F(x,y) = F_0(y) + Et^2\sum_{p=0}^{\infty}\sum_{q=0}^{\infty}\phi_{pq}\cos\left(\frac{p\pi x}{a}\right)\cos\left(\frac{2q\pi y}{b}\right) \tag{6}$$

Substituting Eqs. (5) and (6) into Eq. (1b), we obtain the expression of ϕ_{pq} in terms of a_{mn} and b_{mn} as

$$\frac{8(p^2+4\alpha^2q^2)^2}{\alpha^2}\phi_{pq} = \sum_{m=1}^{\infty}\sum_{n=1}^{\infty}\sum_{i=1}^{\infty}\sum_{j=1}^{\infty}(a_{mn}b_{ij}+b_{mn}a_{ij}+b_{mn}b_{ij}) \cdot\left[2mnij \pm (m^2j^2+n^2i^2)\right] \tag{7}$$

$$-:\begin{cases} p=m+i & \text{and} \quad q=(n+j)/2 \\ \text{or} & \\ p=|\,m-i\,| & \text{and} \quad q=|\,n-j\,|/2 \end{cases}$$

$$+:\begin{cases} p=|\,m-i\,| & \text{and} \quad q=(n+j)/2 \\ \text{or} & \\ p=m+i & \text{and} \quad q=|\,n-j\,|/2 \end{cases}$$

where p and q are positive integers, and α is the aspect ratio of a panel; i.e. $\alpha \equiv a/b$. The final equation to be solved with Eq. (7) can be obtained by the direct substitution of Eqs. (5) and (6) into Eq. (1a), but it turned out to be so complicated that Galerkin's method is applied to Eq. (1a) in the form as

$$f_{rs}(b_{mn},\lambda) \equiv \int_0^a\int_0^b\left\{\nabla^4 w - \frac{t}{D}\left[\frac{\partial^2 F}{\partial y^2}\frac{\partial^2(w+w_0)}{\partial x^2} + \frac{\partial^2 F}{\partial x^2}\frac{\partial^2(w+w_0)}{\partial y^2} - 2\frac{\partial^2 F}{\partial x\partial y}\frac{\partial^2(w+w_0)}{\partial x\partial y}\right]\right\} \cdot\sin\left(\frac{r\pi x}{a}\right)\sin\left(\frac{s\pi y}{b}\right)dxdy = 0, \quad r,s,m,n = 1,2,3,\cdots \tag{8}$$

where w is a function of b_{mn} by Eq. (5). Moreover, these equations can be rewritten as

$$f_{rs}(b_{mn},\lambda) = f_{rs}(b_{11},b_{12},\cdots,b_{mn},\cdots,b_{uv},\lambda) = 0, \quad r,m = 1,\cdots,u, \quad s,n = 1,\cdots,v \tag{9}$$

where $\lambda\,(\equiv M/D)$ is the loading parameter of the applied bending moment, and u, v are the maximum number of modes involved in calculating the out-of-plane deflection assumed by Eq. (5). By substituting Eqs. (5) and (6) into Eq. (8) and integrating it, we obtain a set of the third-order simultaneous algebraic equations of b_{mn}. The substitution of the obtained b_{mn}s into Eq. (5b) yields the out-of-plane deflection in the post-buckling state.

(3) Rectangular plate clamped at two opposite sides and simply-supported along the other two sides

The out-of-plane deflections are assumed to be given by the same shape function as those used by Moriwaki and Nara[25] as

$$w_0 = t\sum_{m=1}^{\infty}\sum_{n=1}^{\infty} a_{mn}\sin\left(\frac{m\pi x}{a}\right) \cdot\left\{\cos\left[\frac{(n-1)\pi y}{b}\right]-\cos\left[\frac{(n+1)\pi y}{b}\right]\right\}, \quad (10a)$$

$$w = t\sum_{m=1}^{\infty}\sum_{n=1}^{\infty} b_{mn}\sin\left(\frac{m\pi x}{a}\right) \cdot\left\{\cos\left[\frac{(n-1)\pi y}{b}\right]-\cos\left[\frac{(n+1)\pi y}{b}\right]\right\} \quad (10b)$$

In this case, the general expression of $F(x,y)$ must satisfy the boundary condition of Eq. (3) and is chosen to be

$$F(x,y) = F_0(y) + Et^2\sum_{p=0}^{\infty}\sum_{q=0}^{\infty}\phi_{pq}\cos\left(\frac{2p\pi x}{a}\right)\cos\left(\frac{2q\pi y}{b}\right) \quad (11)$$

Substituting Eqs. (10) and (11) into Eq. (1b), we obtain the explicit expression for ϕ_{pq}, as well as Eq. (7). Similar to Eq. (8), Galerkin's method is employed to solve Eq. (1a) in the form as

$$f_{rs}(b_{mn},\lambda) \equiv \int_0^a\int_0^b\left\{\nabla^4 w - \frac{t}{D}\left[\frac{\partial^2 F}{\partial y^2}\frac{\partial^2(w+w_0)}{\partial x^2} + \frac{\partial^2 F}{\partial x^2}\frac{\partial^2(w+w_0)}{\partial y^2} - 2\frac{\partial^2 F}{\partial x\partial y}\frac{\partial^2(w+w_0)}{\partial x\partial y}\right]\right\} \cdot\sin\left(\frac{r\pi x}{a}\right)\left\{\cos\left[\frac{(s-1)\pi y}{b}\right]-\cos\left[\frac{(s+1)\pi y}{b}\right]\right\}dxdy = 0, \quad r,m = 1,\cdots,u, \quad s,n = 1,\cdots,v \quad (12)$$

By substituting Eqs. (10) and (11) into Eq. (12) and integrating it, we also obtain a set of the third-order simultaneous algebraic equations of b_{mn}. This explanation is limited to the out-of-plane deflection, and we suggest to refer to the paper[15] with respect to the boundary conditions of in-plane deformation beyond buckling.

3. NUMERICAL CALCULATION BY NEWTON-RAPHSON METHOD

The nonlinear equations of (9) are solved by the perturbation method of the first order; i.e. Newton-Raphson method.

(1) Load-control type method

Consider the reference point (b^0_{mn},λ^0) on the equilibrium path and a foregoing point $(b_{mn},\lambda)=(b^0_{mn}+\Delta b_{mn},\lambda^0+\Delta\lambda)$ with an increment $(\Delta b_{mn},\Delta\lambda)$. We apply the Taylor expansion to Eq. (9), and neglect the higher term more than second order to arrive at a set of linear equation as

$$\left[f^0_{rs,b_{mn}}\right]\{\Delta b_{mn}\} + \left\{f^0_{rs,\lambda}\right\}\Delta\lambda = \{0\} \quad (13)$$

where

$$\left[f^0_{rs,b_{mn}}\right] \equiv \sum_{m=1}^{u}\sum_{n=1}^{v}\left.\frac{\partial f_{rs}}{\partial b_{mn}}\right|_0, \qquad \left\{f^0_{rs,\lambda}\right\} \equiv \left.\frac{\partial f_{rs}}{\partial\lambda}\right|_0$$

if a load increment $\Delta\lambda = \Delta\bar{\lambda}$ is given, the unknown quantities $\{\Delta b_{mn}\}$ are solved by

$$\{\Delta b_{mn}\} = -\left[f^0_{rs,b_{mn}}\right]^{-1}\left\{f^0_{rs,\lambda}\right\}\Delta\bar{\lambda} = -\left[f^0_{rs,b_{mn}}\right]^{-1}\left\{f^0_{rs}(b^0_{mn},\lambda^0+\Delta\bar{\lambda})\right\} \quad (14)$$

As a result, of this (t+1)st approximated coefficients $\{b^{t+1}_{mn}\}$ $(t=0,1,\cdots)$ are obtained as

$$\{b^{t+1}_{mn}\} = \{b^t_{mn}\} + \{\Delta b^t_{mn}\} = \{b^t_{mn}\} - \left[f^t_{rs,b_{mn}}\right]^{-1}\{f^t_{rs}\} \quad (15)$$

where

$$\{f^t_{rs}\} = \{f_{rs}(b^t_{11},b^t_{12},\cdots,b^t_{mn},\cdots,b^t_{uv},\lambda^0+\Delta\bar{\lambda})\}, \qquad \lambda^0+\Delta\bar{\lambda} = \text{const.}$$

Therefore, the determinant of the tangential stiffness matrix just after converged is defined as

$$|K_b| \equiv \left|f^t_{rs,b_{mn}}\right|_{\text{converged}} \quad (16)$$

(2) Displacement-control type method

In the displacement-control type method, the unknowns in the equation are $\Delta\lambda$ and $\{b_{mn}\}$ except for the certain coefficient b_{kl}. After all, the total degree of freedom is the same as those of the load-control method. We, therefore can rearrange Eq. (13), and known quantity $\Delta\bar{b}_{kl}$ is replaced with the unknown quantity $\Delta\lambda$ as

$$\left[{}^{\lambda}f^0_{rs,b_{mn}}\right]\left\{\Delta^{\lambda}b_{mn}\right\} + \left\{f^0_{rs,b_{kl}}\right\}\Delta\bar{b}_{kl} = \{0\} \quad (17)$$

where unknown quantities $\left\{\Delta^{\lambda}b_{mn}\right\}$ can be expressed by

$$\left\{\Delta^{\lambda}b_{mn}\right\} = \{\Delta b_{11},\Delta b_{12},\cdots,\Delta\lambda,\cdots,\Delta b_{uv}\}^{\mathrm{T}} = -\left[{}^{\lambda}f^0_{rs,b_{mn}}\right]^{-1}\left\{f^0_{rs,\bar{b}_{kl}}\right\}\Delta\bar{b}_{kl} = -\left[{}^{\lambda}f^0_{rs,b_{mn}}\right]^{-1}\left\{f^0_{rs}(b^0_{mn},b^0_{kl}+\Delta\bar{b}_{kl},\lambda^0)\right\} \quad (18)$$

where $\{\ \}^T$ means the transpose of matrix. As a result, of this (t+1)st approximated value $(t=0,1,\cdots)$ can be expressed as

$$\left\{{}^{\lambda}b^{t+1}_{mn}\right\} = \left\{{}^{\lambda}b^t_{mn}\right\} - \left[{}^{\lambda}f^t_{rs,b_{mn}}\right]^{-1}\{f^t_{rs}\} \quad (19)$$

where

$$\{f^t_{rs}\} = \{f_{rs}(b^t_{11},b^t_{12},\cdots,b^0_{kl}+\Delta\bar{b}_{kl},\cdots,b^t_{uv},\lambda^t)\}, \qquad b^0_{kl}+\Delta\bar{b}_{kl} = \text{const.}$$

Similarly, the determinant of the tangential coefficient matrix after convergence is defined by

$$|K_\lambda| \equiv \left|{}^{\lambda}f^t_{rs,b_{mn}}\right|_{\text{converged}} \quad (20)$$

4. METHOD OF CLASSIFICATION OF SINGULAR POINTS

(1) Method to employ both $|K_b|$ and $|K_\lambda|$

Singular points on the equilibrium path obtained by solving Eq. (9) are classified by monitoring the determinant of tangential stiffness matrix $[K_b]$ for the load-control method, or the one of tangential coefficient matrix $[K_\lambda]$ for the displacement-control method. The uniqueness of the solution is evaluated from the value of the determinant defined by Eqs. (16) and (20), and the singular points on the equilibrium path are classified[19)~21)]. Here, simple non-degenerate bifurcation points are only considered. On the smoothly increasing or decreasing equilibrium path, only one displacement corresponds to one loading level and vice versa. Therefore, the uniqueness of solution is assured for both cases, and results to $|K_b| \neq 0$ and $|K_\lambda| \neq 0$.

a) Limit point

There is no equilibrium state in the upper loading level of a limit point, but two solutions exist in the lower range, and hence the uniqueness of the solution does not hold for either cases. However, from the viewpoint of displacement, the only one loading level corresponds to a certain displacement. Therefore, $|K_b| = 0$, but $|K_\lambda| \neq 0$ is concluded.

b) Bifurcation point

At a bifurcation point, the uniqueness of solution is not satisfied for both displacement and loading level. Namely, the determinants of tangential matrices for both method become simultaneously singular, that is $|K_b|=|K_\lambda|=0$.

As a result, the relationships between the type of singular point and the value of determinant of tangential matrices; i.e. $[K_b]$ and $[K_\lambda]$, are as tabulated in **Table 1**.

(2) Method to employ $|K_b|$ and eigen vector of $[K_b]$

Assuming $\{e\}$ to be the eigen vector of $[K_b]$, the equilibrium points are classified into the following category[26)]:

$$\begin{cases} |K_b| \neq 0 & \text{ordinary point} \\ = 0 & \text{singular point} \\ \quad \rightarrow \begin{cases} \{f_{rs,\lambda}\}^T\{e\} = 0 & \text{bifurcation point} \\ \neq 0 & \text{limit point} \end{cases} \end{cases} \tag{21}$$

where $\{f_{rs,\lambda}\}$ is called the loading mode vector.

Table 1 Classification of singular points

	$\lvert K_b\rvert$	$\lvert K_\lambda\rvert$
ordinary point	$\neq 0$	$\neq 0$
limit point	$= 0$	$\neq 0$
bifurcation point	$= 0$	$= 0$

5. SEARCH OF EQUILIBRIUM PATH AND CLASSIFICATION OF SINGULAR POINTS

(1) Simply-supported rectangular plate

The equilibrium paths of a simply-supported (4s.s.) rectangular plate obtained by the load-control method are shown in **Fig.2**. It is to be noted that the two symmetrical paths branching from the bifurcation point with opposite sign exist according to both sides of a plate, but this figure includes only one of them. Here, the aspect ratio of a plate is set to be α=0.8 so that the first buckling mode of one half-wave can be obtained for the sake of simplicity. Although the width-thickness ratio is assumed to be β=200, the results are all expressed in terms of non-dimensionalized quantities.

Solid lines indicate the equilibrium points on which the determinant of tangential stiffness matrix $[K_b]$ is positive, while broken lines show those of negative. A dashed-and-dotted line indicates the abrupt jump of equilibrium paths. The load-deflection curves at the point (1); i.e. (0.35a,0.70b) as shown in **Fig.1** are plotted for different equilibrium states. The notation m in **Fig.2** means that the principal mode of m among all components of b_{mn} dominates the bifurcation paths, in other words, m-th order of half sine wave in the x-direction is the principal component of the deflection. In this analysis, u=v=6 of maximum order of modes are adopted for the efficiency requirement of calculation, it may be necessary to take higher order for larger deformation.

The bifurcation path of the principal mode m=1 starts from point A, and the out-of-plane deflection gradually begins to grow with other minor modes of m=3,5 as the applied moment increases. The out-of-plane deflection of point (1) has the maximum value in the vicinity of loading level M/D=100, but decreases after that. An instability phenomena thought to be the secondary buckling occurs at point B, and bifurcation path jumps to point D. This point D lies exactly on the path of principal and single mode of m=3.

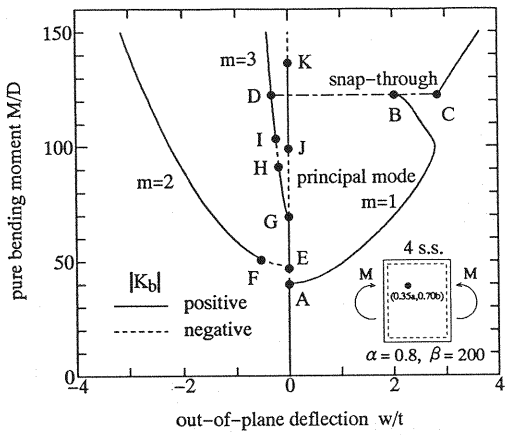

Fig. 2 Equilibrium paths for 4s.s. obtained by load-control method and the sign of $|K_b|$

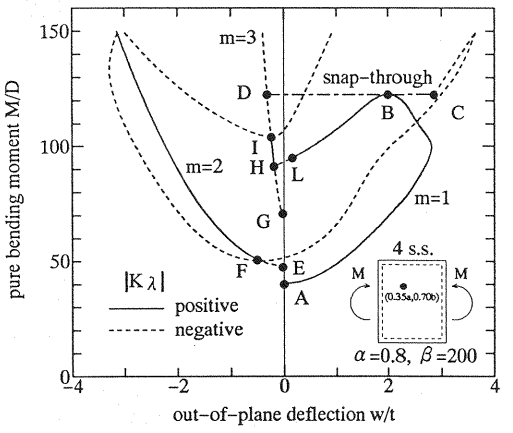

Fig. 3 Equilibrium paths for 4s.s. obtained by displacement-control method and the sign of $|K_\lambda|$

Moreover, the equilibrium path also jumps into another unstable one indicated by point C with m=1,3,5, but it ceases to continue smoothly from the preceding stable path of A→B.

If point B is the limit point on the path of principal m=1, we can expect that some unstable paths surely exist in the vicinity of point B. But in this load-control analysis, the unstable path followed by point B can not be searched, thereby we can not certify the physical inevitably of this jumping phenomenon at this stage of the research.

The bifurcation path of m=2 starts from point E and gradually grows, but the deformation mode interact with a higher mode m=6. Similarly, the path of single mode of m=3 increases monotonically from point G. In this figure, the ordinate w/t=0 expresses the trivial solution, and the points A,E,G,J,K are obtained as the singular points on this axis. In fact, the bifurcation paths from points A,E,G are traced and plotted in the figure.

The numerical results obtained by the displacement-control method are shown in **Fig.3**. In the case of the displacement-control analysis, since the determinant and eigen value of the tangential stiffness matrix $[K_b]$ can be obtained in advance of those of tranformed $[K_\lambda]$, the checking operation of the determinant is quite easy and systematic.

The determinant of the tangential coefficient matrix $[K_\lambda]$ is also distinguished by the sign. By using the displacement-control analysis, equilibrium paths beyond point B can be obtained, and this point B is identified as the limit point. The

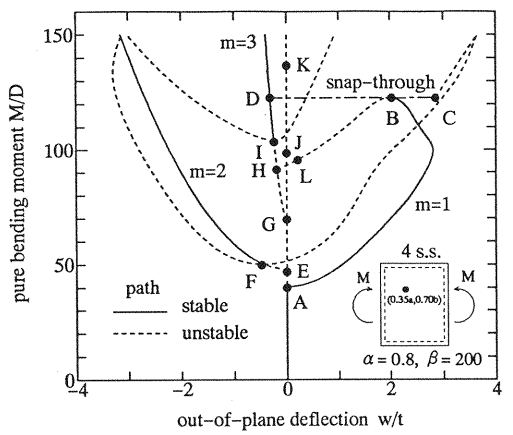

Fig. 4 Instability of equilibrium paths for 4s.s. boundary condition

out-of-plane deflection decreases after point B, and the path reaching to point H crossing the axis w/t=0 can be traced. The determinant of path B–H changes its sign from positive to negative at the intermediate point L, and the principal mode m=1 varies gradually to single m=3 correspondingly. Namely, this L–H path can be interpreted as the mode transition process from principal m=1 to single m=3.

The bifurcation paths from points I,F are searched and plotted as broken lines. The equilibrium state is composed of all modes of b_{mn} in these bifurcated paths, hence the symmetry of the system is completely lost. It is notewor-

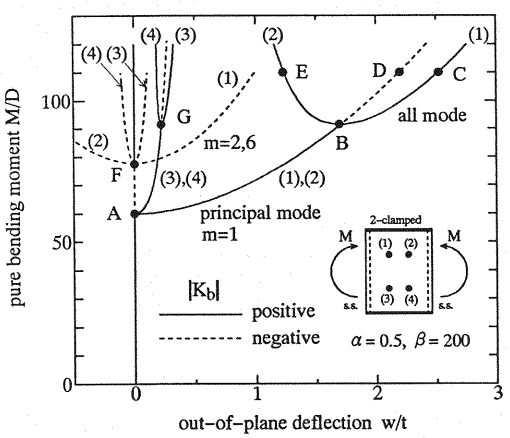

Fig. 5 Equilibrium paths obtained by load-control method for 2c. & 2s.s. boundary condition

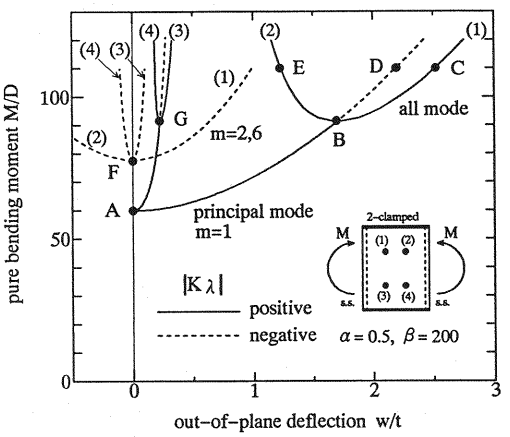

Fig. 6 Equilibrium paths obtained by displacement- control method for 2c. & 2s.s. boundary condition

thy that the load-control method must be employed on the ordinate w/t=0, because, in the case of displacement-control analysis, determinant becomes zero on this axis.

Referring to both **Figs.2** and **3**, we classify the singular points based on **Table 1**. At first, it is found that the point B is a limit point. The points F,H,I have turned out to be scondary bifurcation points, in addition to the primary buckling point A,E,G (we can not judge by $|K_\lambda|$). Since the sign of the determinants of both K_b and K_λ also changes at point L, this is a bifurcation point, but the bifurcation path from the point L are not found in this paper.

As mentioned above, the singular points on the equilibrium paths can be classified, but it must be noted that the sign of determinant of the tangential matrix is not sufficient index to decide the instability of their paths. The necessary conditions that the equilibrium path is stable are as follows: (1) determinant of the tangential stiffness matrix is positive, (2) all eigen values of the tangential stiffness matrix are positive. The former is the necessary condition that the energy surface of the system becomes convex in the downward, and the later is the necessary and sufficient condition. **Fig.4** shows the re-drawn solid lines which denote the stable paths fulfilling the positive-definite requirements of the tangential stiffness matrix.

Since the paths E–G,G–H,J–K have the negative eigen values of even number, the determinant of the overall matrix becomes positive apparently as shown in **Fig.2** . However, the true stable equilibrium paths are found to be 0–A–B,F+,I–D+ as shown in **Fig.4**, in which the notation '+' stands for the production path in the higher loading level.

As a consequence, it is concluded that the possible equilibrium path of a plate with an infinitesimal initial imperfection is 0–A–B–D+ only.

(2) Rectangular plate clamped at two opposite sides and simply-supported along the other two sides

In this case, the load-control and displacement-control methods have similar results. Their equilibrium paths are shown in **Figs.5** and **6**. We here focuses on two points (1)(0.35a,0.70b) and (2)(0.65a,0.70b) in **Fig.1**.

The primary buckling occurs at point A in the vicinity of the loading level M/D=60, and the post-buckling configuration is composed of the principal modes of m=1 with 3,5. After that, out-of-plane deflection increases smoothly with the increase of the loading, but the secondary instability due to bifurcation occurs at point B of M/D=90.

The deflection of point (1) increases monotonically, while that of point (2) decreases. The configuration mode of odd numbers m=1,3,5 up to point B changes to the all mixed one; i.e. the symmetry of this system with respect to y-axis vanishes. Since the deflection of points (3) and (4) of tension sides also shows the unsymmetrical configuration, point G is the secondary buckling point, like the point B. Moreover, the unstable path B–D+ on the production of A–B is also found. The primary buckling point F of higher mode and the bifurcation paths from here are also

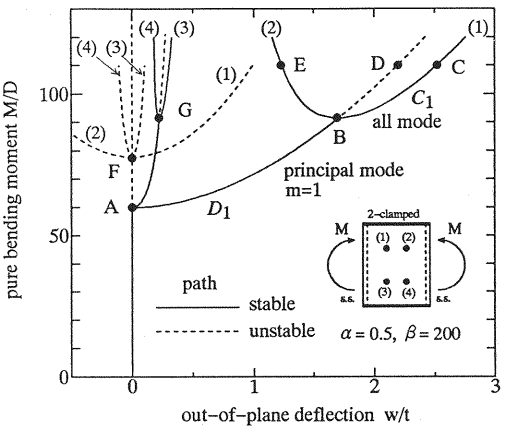

Fig. 7 Instability of equilibrium paths for 2c. & 2s.s. boundary condition

searched.

From these figures, with reference to the sign of determinant of the tangential matrix $[K_b]$, $[K_\lambda]$ and referring to **Table 1**, it can be identified that the bifurcation points are B,G and A,F on the w/t=0 axis. Furthermore, the possible stable equilibrium path is concluded to be A–B–C+ and A–B–E+ as shown in **Fig.7**.

6. GROUP-THEORETIC BIFURCATION THEORY

(1) Application of block-diagonalization technique

We now block-diagonalize the tangential stiffness matrix $[f_{rs,bmn}]$ for the simply-supported (4s.s.) plate as mentioned in chapter **3**. This matrix is denoted by $[J_\ell]$, and the subscript ℓ stands for the number of principal mode of equilibrium paths; i.e. m=ℓ. The tangential stiffness matrix is block-diagonalized by the coordinate transfer matrix H[18] which implements the properties of the symmetry of the structural system as follows:

$$\left[\tilde{J}_1\right] = H^{\mathrm{T}}[J_1]\,H = \begin{bmatrix} \left[\tilde{J}_1^{(315)}\right] & 0 \\ 0 & \left[\tilde{J}_1^{(426)}\right] \end{bmatrix}, \quad (22a)$$

$$\left[\tilde{J}_2\right] = H^{\mathrm{T}}[J_2]\,H = \begin{bmatrix} \left[\tilde{J}_2^{(315)}\right] & & 0 \\ & \left[\tilde{J}_2^{(4)}\right] & \\ 0 & & \left[\tilde{J}_2^{(26)}\right] \end{bmatrix}, \quad (22b)$$

$$\left[\tilde{J}_3\right] = H^{\mathrm{T}}[J_3]\,H = \begin{bmatrix} \left[\tilde{J}_3^{(3)}\right] & & & 0 \\ & \left[\tilde{J}_3^{(15)}\right] & & \\ & & \left[\tilde{J}_3^{(42)}\right] & \\ 0 & & & \left[\tilde{J}_3^{(6)}\right] \end{bmatrix} \quad (22c)$$

In this analysis, the block-diagonalization is accomplished simply by the rearrangement of the rows and columns of $[J]$, because the shape functions of the deflection are given by the Fourier series. Here, $[\tilde{J}_m^{(ij\cdots)}]$ of the right-hand-side of Eq. (22) indicates the diagonal block composed of modes $i, j, \cdots$.

By applying the block-diagonalization principle,$[\tilde{J}_i]$ becomes sparse, and the main path can be searched only by the relevant condense block. Bifurcation phenomena can be understood as the mixing of the mode for main path and that for bifurcation path through the mode interaction. $[\tilde{J}_1^{(315)}, \tilde{J}_2^{(26)}], \tilde{J}_3^{(3)}]$ are the main blocks expressing the main path for m=1,2,3, respectively.

Other blocks or sub-matrices in the block-diagonalized stiffness matrix also give the bifurcation paths. Generally, the limit point is expressed by the one at which the main block becomes singular, and bifurcation occurs when the determinant of the other block becomes zero. The bifurcation path retains the symmetry of its singular block[27].

The symmetric group of each diagonal block in Eqs. (22a)~(22c) is as follows:

$$\sum\left(\tilde{J}_1^{(315)}\right) = D_1,\ \sum\left(\tilde{J}_1^{(426)}\right) = C_1,$$
$$\sum\left(\tilde{J}_2^{(315)}\right) = C_1,\ \sum\left(\tilde{J}_2^{(4)}\right) = C_2,\ \sum\left(\tilde{J}_2^{(26)}\right) = D_2,$$
$$\sum\left(\tilde{J}_3^{(3)}\right) = D_3,\ \sum\left(\tilde{J}_3^{(15)}\right) = D_1,$$
$$\sum\left(\tilde{J}_3^{(42)}\right) = C_1,\ \sum\left(\tilde{J}_3^{(6)}\right) = C_3 \quad (23)$$

where $\sum(\cdot)$ denotes the group representing the symmetry of the matrix inside the parentheses. D_m stands for the dihedral group having the m-axis symmetry, and C_n denotes the rotation group with rotational symmetry of the angle of $2n/\pi$.

Moreover, the bifurcation diagram degenerated by the boundary conditions is shown in **Fig.8** for both cases of simply-supported (4s.s.) and of two opposite sides clamped and other two sides simply-supported (2c. & 2s.s.) boundary conditions. The same bifurcation diagram is applicable to these boundary conditions. Here, D_∞ indicates the symmetric group of circles and, simultaneously, the symmetry of the trivial solution of w/t=0. This bifurcation diagram offers a complete rule of bifurcation for a D_∞-equivalent system. For example, A→B

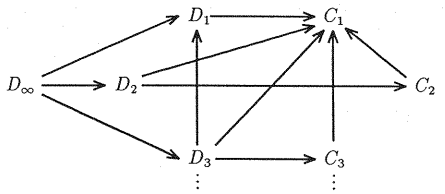

Fig. 8 Diagram of bifurcation hierarchy for D_∞-invariant system

means that B-invariant solution bifurcates from A-invariant one. However, in the actual physical phenomena, B-invariant solution may return to A-invariant main path in some cases. These bifurcation processes can be understood as a natural consequence of hierarchical bifurcation[18].

(2) Classification of bifurcation point by group-theoretic bifurcation theory

Fig.9 shows the sign of the determinant of each diagonal block in the block-diagonalized matrix for all equilibrium paths. As above mentioned, the solid and broken lines denote the stable and unstable paths, respectively.

The bifurcation paths for principal m=1,2,3 from the trivial axis w/t=0 have the symmetry of D_1,D_2,D_3, respectively. Based on similar consideration, it is guessed that the bifurcation paths from points J,K as referred in chapter **5 (1)** also have the symmetry of D_4,D_5, and the principal mode of their bifurcation paths will become m=4,5, respectively.

The symmetries of blocks on the path of m=2 are labeled by D_2,C_2,C_1. The main path is expressed by D_2 which is composed of $\left[\tilde{J}_2^{(26)}\right]$ with symmetric modes of m=2,6. The determinant of a block for C_1 becomes zero (singular) at point F, and hereafter the bifurcation path C_1 branches. In this way, the singular points can be classified by checking the block which becomes singular.

The main path of m=3 is expressed by the block with symmetry D_3, but the sign of determinant changes at points H,I in some blocks. The symmetry of this path is found to be D_3,D_1,C_3,C_1, and C_1-invariant path bifurcates from point I as shown in figure. Furthermore, D_1-invariant path branches from point H and finally connects with the main path of principal m=1.

In the principal m=1 path, the bifurcation occurs at point A from the trivial axis w/t=0. A block for this path has the symmetry of D_1 corresponding to the main path and C_1 for the bifurcation path, respectively. After point B, there exist the transition paths of B→D+ and descending path of B–H. In the path A–B–L, the determinant of main block $\left[\tilde{J}_1^{(315)}\right]$ changes its sign into negative at point B only, and returns to positive in the path B–L.

In this way, the singularity of the main block in a block-diagonalized matrix suggests the existence of a limit point, and the descending path B–H can be expected. Although it is not actually found in this analysis, the branching path from the intermediate bifurcation point L on the B–H path is expected to have the symmetry of C_1 from the property of block-diagonalized matrix. Furthermore, on the other path of B→C+, C_1 block which expresses the bifurcation path becomes simultaneously singular, and complicated behaviors with maintaining the symmetry of D_1 are derived. It can be similarly understand as the bifurcation hierarchy shown in **Fig.7** by the process of $D_\infty \rightarrow D_1 \rightarrow C_1$.

As mentioned above, the block-diagonalization operation makes it possible to trace the main path easily by using only the main block of the transformed matrix. If we previously know the bifurcation hierarchy and the bifurcation diagram for the structural systems by means of the group theory, the foresighted bifurcation analysis can be carried out with the aid of the block-diagonalization technique.

In other words, the bifurcation diagram can be called as a signpost which represents correctly the bifurcation hierarchy of the system. Therefore, the mechanism of the bifurcation is already expressed explicitly by the bifurcation diagram as shown in **Fig.8** even for the complicated problems such as the post-buckling behavior of an elastic plate. However, the actual interestings, such as when the bifurcation occurs, or which bifurcations occur faster, are dependent on the individual problems for each structural system, and there is no way to know except for carrying out the actual numerical calculations.

7. EFFECT OF INITIAL IMPERFECTION

In this chapter, the influence of the initial imperfection on the post-buckling behavior of a plate is investigated from the diversified points of view.

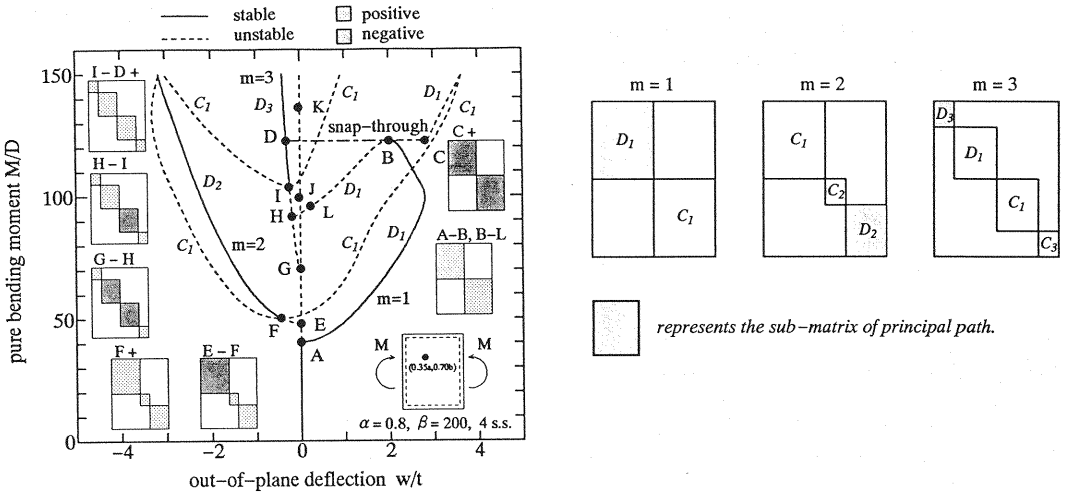

Fig. 9 Determinant $|\tilde{J}|$ of equilibrium paths and block-diagonalized matrices

(1) Imperfection sensitivity laws in the vicinity of stable-symmetric bifurcation point

As the quantitative evaluation method of initial imperfection, the 2/3rd power law by Koiter[28] is well known, but physically-meaningless information is obtained for the stable-symmetric bifurcation points such as point A in **Fig.9**. Accordingly, we here adopt the imperfection sensitivity laws[23),24)], which is applicable for the stable-symmetric bifurcation points, to evaluate quantitatively the influence of the initial imperfection.

As an example of stable-symmetric bifurcation points, the post-buckling analysis[24)] for the simply-supported rectangular plate as shown in **Fig.1** are carried out. Assuming the initial out-of-plane deflection of magnitude $a_{11}=\varepsilon<0.4$, the observation point of non-dimensionalized deflection $\bar{w} \equiv (w + w_0)/t$ is set to be $(0.5a, 0.7b)$. **Fig.10** shows the load-deflection curves for various magnitude ε of initial imperfection. These curves can be approximated asymptotically by the following bifurcation equation[22),23)]:

$$\bar{w}\tilde{f} + p\bar{w}^3 + q\varepsilon + \text{higher order terms} = 0 \qquad (24)$$

in the vicinity of the bifurcation point. $\tilde{f} \equiv \Delta M/D$ indicates the load increment from the bifurcation point, and p, q are constants. A parabola curves of

$$\tilde{f} = -g\bar{w}^2 \qquad (25)$$

(g=40.25, 40.25×4) are drawn from the bifurcation point in the same figure. The value of deflection $\hat{w} \equiv \bar{w}|_{\tilde{f}=-g\bar{w}^2}$ at which these parabola intersect the load-deflection curves of Eq. (24) obeys the following 1/3rd power law:

$$\hat{w} = K^{1/3}\varepsilon^{1/3} + \mathrm{O}(\varepsilon) \qquad (26)$$

The higher imperfection sensitivity is recognized; i.e. deflection largely varies even for the small change of initial imperfection, in which

$$K = \frac{q}{g-p} \qquad (27)$$

Although it seems to be strange to evaluate the deflection on the parabola (25), the deflection at buckling for the perfect system can be evaluated by putting g=0; i.e. $\tilde{f}$=0. The relationships between the deflection $\hat{w}$ at the intersecting points in **Fig.10** and the 1/3rd power of the initial imperfection are presented in **Fig.11**. Linearity of the relation is surely recognized, and hence an asymptotic equation (26) is justified. The approximated values of deflection by the bifurcation equation (24) are plotted by the symbol (×) in **Fig.10**. Good agreement of these approximated values with analytical ones represented by solid lines is recognized. The influence of initial imperfection in the vicinity of the stable-symmetric bifurcation points can be evaluated quantitatively in this manner.

Next, we investigate the stochastic fluctuation of $\hat{w}$ when each of imperfection variables $(d_1, \cdots, d_p)$ has the normal distribution with zero average. From Ref. 29), the variable K of Eq. (26) is expressed by

$$K = \sum_{i=1}^{p} c_i d_i \qquad (28)$$

as a function of imperfection variables, in which c_i are constants. The variable K also obeys the normal distribution with zero average and variance σ, because the sum of normal distribution is also normal distribution. The probability density function $f_{\hat{w}}(\hat{w})$ of variable $\hat{w}$ in the left-hand-side

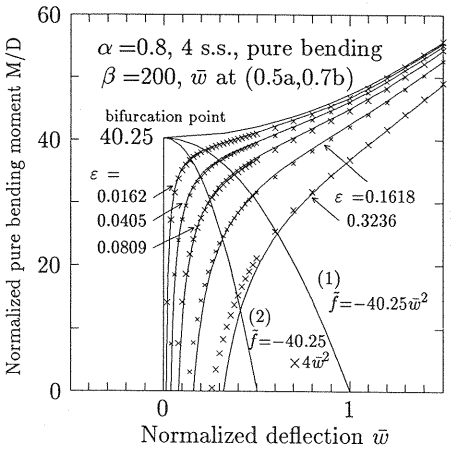

Fig. 10 Equilibrium paths in the vicinity of stable-symmetric bifurcation point and their asymptotic approximations (parabola from the bifurcation point is given by Eq. (25))

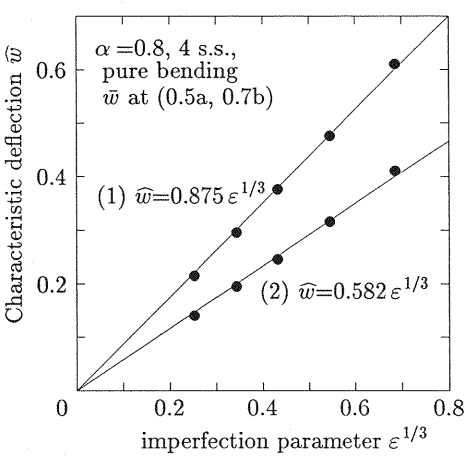

Fig. 11 Relationships between $\hat{w}$ and $\epsilon^{1/3}$

of Eq. (26) is obtained as

$$f_{\hat{w}}(\hat{w}) = f_K(K)\frac{\mathrm{d}K}{\mathrm{d}\hat{w}} = \frac{3\hat{w}^2}{\sqrt{2\pi}\hat{\sigma}}\exp\left(-\frac{\hat{w}^6}{2\hat{\sigma}^2}\right), \quad (-\infty < \hat{w} < \infty) \tag{29}$$

by the variable transformation of the probability density function for K, in which $\hat{\sigma} = \sigma\varepsilon$. Since the assumption that imperfection variables $(d_1, \cdots, d_p)$ obey the normal distributions with zero average is relatively valid in view of the central limit theorem, Eq. (29) seems to give good approximation for the probability density of $\hat{w}$.

(2) Imperfection sensitivity laws in the vicinity of relative maximum and/or minimum point of deflection

Since we can deal with the deflection and loading parameter as the essentially equivalent independent variable, the relative maximum and minimum points of deflection can be handled equally with those of loading. By the previous studies[29] about relative maximum and minimum points of loading, it is found that the extremum points of deflection have the low imperfection sensitivity in proportion to ε and their values also obey a normal distribution.

(3) Monte Carlo simulation

Monte Carlo simulation is carried out to investigate quantitatively the influence of the initial imperfection assuming the normalized random number with zero average and variance of unity as the magnitude of imperfection mode a_{mn}. Five kinds of imperfection patterns and four cases of magnitude 1/100, 2/100, 5/100, 1/10 of a_{mn} are considered. Representative examples of equilibrium path obtained are shown in **Fig.12**

Various equilibrium paths are obtained for those imperfections, but they gather in the vicinity of either paths of principal m=1,2,3. Especially in the case of small imperfections, the snap-through phenomena also occur almost the same loading level as the secondary buckling of principal m=1 path. In these cases, the branch switching to other paths and the mechanism of snap-through are categorized into following three cases:

1) main path O–A switches to A–B, and snaps to point D from B,
2) main path O–A switches to A–B, and snaps to isolated point C from B,
3) main path O–A switches to E–F.

The results of simulation show that the case 1) occurs most frequently, but other two cases seldom happen. The case 2) means the occurrence of snap-through to isolated solution, and this informs us the limit of current methodology of bifurcation analysis for tracing carefully the equilibrium path connected to origin. This is the reason to develop the other method[30] by which the isolated solutions are directly traced.

The bifurcation rules for these three cases is expressed by

$$\begin{array}{l} D_\infty \Rightarrow D_1 \Rightarrow D_3 \\ D_\infty \Rightarrow D_1 \Rightarrow D_1 \\ D_\infty \Rightarrow D_2 \end{array} \tag{30}$$

where $\Rightarrow$ stands for the branching or snap-through to other paths. It is found that they

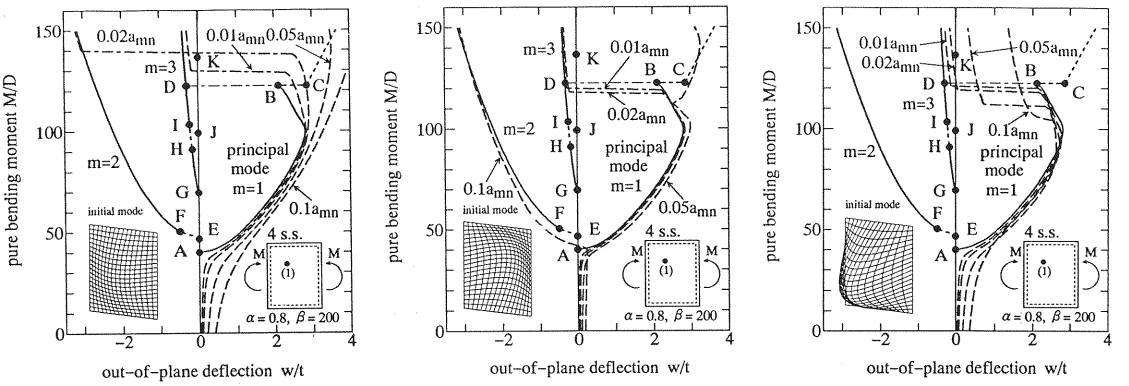

Fig. 12 Relationships between initial imperfection and equilibrium path in Monte Calro simulation

all obey the bifurcation diagram as shown in **Fig.8**. It is natural that the path branching obeys this diagram, but it is interesting that the snap-through phenomena also keep it. Verification of its generality will be a topic requiring further studies.

In the vicinity of stable-symmetrical bifurcation point A, fluctuation of deflection becomes large for the change of imperfection, while becomes small in the vicinity of the relative maximum point of deflection. This fact assures the validity of asymptotic law introduced in (1),(2) of this chapter. However, it must be noticed that this law is suitable for the local properties in the vicinity of the bifurcation points or relative maximum point of deflection, but can not be applied to the global features such as the snap-through of a path to another. This shows the importance of Monte Carlo simulation carried out in this section to investigate the global behavior of a plate. It is concluded that, in order to evaluate the magnitude of deflection of a plate, an asymptotic law is effective for relatively small deflection, while the post-buckling analysis is necessary for large deflection to make it possible to consider the branch switching and snap-through phenomena.

8. CONCLUSION

The post-buckling analysis is carried out for both the 4s.s. and 2c. & 2s.s. elastic rectangular plates. Numerical classification of the instability points (bifurcation and limit points) on the equilibrium path and the evaluation of deflection are carried out, and the following conclusions are have been attained:

1) After the primary buckling of a 4s.s. rectangular plate subject to pure bending, it is recognized that the snap-through phenomena from the path of principal $m=1$ to single $m=3$ occur, and other bifurcation points also exist. The singular points occurred in a 2c. & 2s.s. plate are identified to be the bifurcation ones. The whole post-buckling behavior of a elastic rectangular plate is revealed numerically in this paper.
2) In order to search the equilibrium path beyond the limit point, the numerical method of both load-control and displacement-control type operations are adopted in this study, and the possible equilibrium paths can be obtained entirely. With the use of these techniques, the bifurcation path from the secondary buckling point are also traced.
3) Group-theoretic bifurcation theory is applied for the post-buckling behavior of a rectangular plate. By applying the block-diagonalization principle to the tangential stiffness matrix, the main route of a equilibrium path can be traced by the block-diagonalized sub-matrix only. It is numerically confirmed that the mechanism of bifurcation surely follows the bifurcation diagram, and the usefulness of this theory is verified.
4) The influence of initial imperfection on the post-buckling behavior is investigated numerically by Monte Carlo simulation. The existence of the snap-through to isolated path and mode switching phenomena of deflection induced by the various imperfection

are revealed, and hence the importance of the post-buckling analysis is emphasized.

5) The post-buckling behavior of a plate is a complicated phenomena including such as secondary buckling, snap-through, and hence the many-sided methodology combining various methods of analysis is necessary to reveal it.

REFERENCES

1) Levy,S.: Bending of rectangular plates with large deflections, *NACA, Technical Notes*, No.846, 1942.
2) Coan, J.M.: Large deflection theory for plates with small initial curvature loaded in edge compression, *J. Appl. Mech.*, Vol.18, pp.143–151, 1951.
3) Yamaki,N.: Postbuckling behavior of rectangular plates with small initial curvature loaded in edge compression, *Trans. ASME, J. Appl. Mech.*, Vol.26, pp.407–414, 1959.
4) Bauer,L. and Reiss,E.L.: Nonlinear buckling of rectangular plates, *J. Soc. Indust. Appl. Math.*, Vol.13, No.3, pp.603–626, 1965.
5) Sharman,P.W. and Humpherson,J.: An experimental and theoretical investigation of simply-supported thin plates subjected to lateral load and uniaxial compression. *Aeronaut. J., Roy. Aeronaut. Soc.*, Vol.72, pp.431–436, 1968.
6) Chilver,A.H.: Coupled modes of elastic buckling. *J. Mech. Phys. Solids*, Vol.15, pp.15–28, 1967.
7) Uemura,M. and Byon O-Il: Secondary buckling of a flat plate under uniaxial compression Part 1: Theoretical analysis of simply supported flat plate. *Int. J. Non-Linear Mech.*, Vol.12, pp.355–370, 1977.
8) Uemura,M. and Byon O-Il: Secondary buckling of a flat plate under uniaxial compression Part 2: Analysis of clamped plate by F.E.M. and comparison with experiments. *Int. J. Non-Linear Mech.*, Vol.13, pp.1–14, 1978.
9) Supple,W.J.: Coupled branching configurations in the elastic buckling of symmetric structural systems. *Int. J. Mech. Sci.*, Vol.9, pp.97–112, 1967.
10) Supple,W.J.: On the change in buckle pattern in elastic structures. *Int. J. Mech. Sci.*, Vol.10, pp.737–745, 1968.
11) Supple,W.J.: Changes of wave-form of plates in the post-buckling range, *Int. J. Solids Structures*, Vol.6, pp.1243–1258, 1970.
12) Nakamura,T. and Uetani,K.: The secondary buckling and post-secondary-buckling behaviours of rectangular plates, *Int. J. Mech. Sci.*, Vol.21, pp.265–286, 1979.
13) Maaskant,R. and Roorda,J.: Mode jumping in biaxially compressed plates, *Int. J. Solids Structures*, Vol.29, No.10, pp.1209–1219, 1992.
14) Fujii,K. and Ohmura,H.: Nonlinear bending behavior of curved girder-web with initial deflections, *J. Struct. Eng., JSCE*, Vol.35A, pp.117–126, 1989 (in Japanese).
15) Nakazawa,M., Iwakuma,T. and Kuranishi,S.: Elastic buckling strength and post-buckling behavior of a panel under unequal bending and shear, *Structural Eng./Earthquake Eng., Proc. of JSCE*, Vol.8, No.1, pp.11s–20s, 1991.
16) Nakazawa,M.: Instability in the post-buckling behavior of a elastic rectangular plate, *8th Symposium on Space Structures*, pp.161–166, 1992 (in Japanese).
17) Nakazawa,M., Iwakuma,T., Kuranishi,S. and Hidaka,M.: Instability phenomena of a rectangular elastic plate under bending and shear, *Int. J. Solids Structures*, Vol.30, No.20, pp.2729–2741, 1993.
18) Ikeda,K., Nakazawa,M. and Wachi,S.: Degeneration of bifurcation hierarchy of a rectangular plate due to boundary conditions, *Proc. JSCE*, No.507/I–30, pp.65–75, 1995 (in Japanese).
19) Hangai,Y. and Kawamata,S.: Bifurcation and snap-through buckling as the eigen problems, *Proc. of Annual Conference, AIJ*, pp.1021–1022, 1971 (in Japanese).
20) Hangai,Y. and Kawamata,S.: Analysis of geometrically nonlinear and stability problems by static perturbation method, *Report of the Institute of Industrial Science*, The University of Tokyo, Vol.22, No.5, Jan., 1973.
21) Edited by JSSC, Naruoka.M. and Nakamura,T.: *Handbook on the Method of Analysis of Frame Structures*, Baifukan, pp.91–117, 1976 (in Japanese).
22) Thompson,J.M.T. and Hunt,G.W.: *A General Theory of Elastic Stability*, John Wiley and Sons, New York, 1973.
23) Ikeda,K. and Goto,S.: Imperfection sensitivity for size effect of granular materials, *Soils and Foundations*, Vol.33, No.2, pp.157–170, 1993.
24) Ikeda,K., Iwakuma,T., Nakazawa,M., Goto,S. and Hori,M.: Asymptotic simulation of bifurcation properties by imperfection sensitivity laws, *J. Struct. Eng., JSCE*, Vol.39A, pp.407–418, 1993 (in Japanese).
25) Moriwaki,Y. and Nara,S.: Buckling strength of web plates of plate girders under in-plane combined loading, *J. Struct. Eng., JSCE*, Vol.35A, pp.127–134, 1989 (in Japanese).
26) Hangai,Y. and Kawaguchi,K.: *Shape Analysis*, Baifukan, pp.141–149, 1991 (in Japanese).
27) Ikeda,K. and Murota,K.: Bifurcation analysis of symmetric structures using block-diagonalization, *Comp. Meth. Appl. Mech. Engrg.*, Vol.86, No.2, pp.215–243, 1991.
28) Koiter, W.T.: On the stability of elastic equilibrium, *Ph.D. Dissertation*, Delft, Holland, 1945. (English translation: NASA Tech. Trans. F10: 833, 1967).
29) Ikeda,K. and Murota,K.: Statistics of normally distributed initial imperfections, *Int. J. Solids Structures*, Vol.30, No.18, pp.2445–2467, 1993.
30) Fujii,F. and Kitagawa,R.: Branching predictor in elastostatic bifurcation, *J. Struct. Eng., JSCE*, Vol.39A, pp.323–332, 1993 (in Japanese).